



# Combined IP/OOP parametric non-linear static analysis on RC frame buildings infilled with strengthened thin masonry panels

Massimiliano Minotto<sup>a,b</sup>, Marco Donà<sup>b,c</sup>, Nicolò Verlato<sup>c</sup>, Enrico Bernardi<sup>c</sup>, Francesca da Porto<sup>d</sup>

<sup>a</sup> Department of Civil, Environmental, Architectural Engineering and Mathematics, University of Brescia, Via Branze 43, 25123 Brescia, Italy

<sup>b</sup> Dept. of Civil, Architectural and Environmental Engineering, University of Padova, Via Marzolo 9, 35131, Padova (IT)

<sup>c</sup> Earthquake Engineering Research & Test Center, University of Guangzhou, Guang Yuan Zhong Rd. 248, 510405, China

<sup>d</sup> Department of Geosciences, University of Padova, Via Gradenigo 6, 35131, Padova (IT)

*Keywords: infilled RC frames; In-Plane and Out-Of-Plane interaction; masonry infill; strengthened masonry; macro-modelling; non-linear analysis*

## ABSTRACT

The use of unreinforced thin clay masonry infills in RC frames as internal partition walls is widespread. Medium and more severe earthquakes are responsible of relevant monetary and human life losses caused by the interaction between the In-Plane and the Out-Of-Plane action that affects these non-structural elements. In order to reduce the Out-Of-Plane vulnerability of these weak panels, three external reinforcing solutions were experimentally investigated at the laboratory of the University of Padova. Such solutions consists of external plaster layers applied both sides of the masonry wall and the additional embedding of a basalt fiber mesh. This paper presents a new macro-model able to predict the combined In-Plane/Out-Of-Plane response of thin masonry infills through two non-linear fiber struts along each diagonal direction. The proposed macro-model was calibrated on the results of combined In-Plane/Out-Of-Plane experimental tests carried out on unreinforced and strengthened thin masonry infills. The aim of the numerical study is the evaluation of the benefits of the proposed reinforcing solutions on the RC infilled frames overall behavior. For this purpose, an extended parametric non-linear static analysis was carried out on RC frames representative of the Italian building stock, both traditionally and seismically designed. Two different incremental In-Plane force patterns were applied on the frame whereas Out-of-Plane equivalent static forces, calculated for three increasing values of Peak Ground Acceleration, were applied directly on the non-structural elements. The analyses were carried out for both types of panels previously calibrated. The evaluation of the strengthening effectiveness is shown in terms of improvement of the overall structural response, postponement of all infill Limit States and thus different damage distribution along building height. Finally, the new Italian Seismic Classification procedure was implemented to evaluate the reduction of the expected annual seismic losses, as well as of the seismic Risk Class.

## 1 INTRODUCTION

The use of thin unreinforced masonry (TURM) infills as enclosure and internal partition walls represents a widespread practice in the construction of Reinforced Concrete (RC) frame buildings all over around the world. The design of masonry infills is affected by several uncertainties, among which their contribution to the lateral stiffness and to the maximum strength of the RC frame. Italian and European Codes classify masonry infills as non-structural elements. It follows that infill walls are often neglected in the current design procedures and their contribution is represented only in terms of

additional masses. It is noteworthy that, also if TURM walls represents light infills system (thickness around 10÷15 cm), their contribution to the lateral response of RC frame structures in terms of stiffness and strength is significant (Dolšek and Fajfar, 2008). The observations on field after seismic events (i.e. L'Aquila, 2009, Italy; Lorca, 2011, Spain; Emilia, 2012, Italy; Kefalonia, 2014, Greece; Central Italy, 2016) confirmed the high seismic vulnerability of the non-structural panels and their typical In-Plane and Out-Of-Plane damages. The deformation of the RC frame induces relevant IP failures at the lower floors (typical X-diagonal cracks) causing a reduction of the masonry OOP strength. The combined IP/OOP seismic action can induce the

partial or total collapse of the infill walls at intermediate storeys (depending on the building height) with subsequent induced soft-storey mechanism. This structural failure mode was observed also in case of RC frame buildings with a regular distribution of masonry panels (Dolšek and Fajfar, 2001). Finally, the infill-frame interaction is responsible of another type of failure that affects the RC structural members, especially in case of existing structures designed only for gravity loads (i.e. '60-'80) in which the confinement of beam-column joints and the reinforcement detailing are poor.

All these typical failure modes, also linked to the lack of a suitable and effective design procedure (Hak et al., 2012), are responsible of relevant economic losses, loss of building functionality and safety issues. In the recent years, many researches focused their attention to the development and the experimental study of adequate strengthening solutions able to control the IP and the OOP damage of the TURM infills and to reduce their intrinsic vulnerability.

Among the first studies, Calvi and Bolognini (2001) tested the combined IP/OOP response of unreinforced and variously reinforced thin masonry panels through full-scale RC infilled frame specimens. The authors proposed, in case of new buildings, the use of the reinforcement in the mortar layers and of light wire meshes in the external plaster to especially improve the OOP infill performance. In the context of the rehabilitation of existing buildings, other authors focused on the application of external reinforcements made of Fibber-Reinforced Plastic (FRP) layers (Tumialan et al., 2003, Saatcioglu et al., 2005) and strengthening meshes, embedded into plaster layers. The use of Textile Reinforced Mortars (TRM) on non-load bearing masonry panels was widely investigated by Calvi et al. (2001), Papanicolau et al. (2007), Valluzzi et al. (2014) and Minotto et al. (2019). It is noteworthy that European standard EN 1998-1-1 recommends adequate interventions on infill panels (slenderness $>15$ ), proposing the use of light wire meshes. A similar prescription was introduced in the more recent Italian Code NTC2018 suggesting the use of light wire meshes to avoid the OOP ejection and a desirable improvement of the Building Risk Class as reported in D.M. 65, 7<sup>th</sup> March 2017.

The influence of masonry infills on the RC frame buildings overall response can be numerically investigated by implementing masonry wall macro-models in RC frame models. In the last decades, many masonry infills macro-models (single diagonal strut and more complex

multi-strut models) were developed (Asteris et al., 2011, Jeselia et al., 2013 and Tarque et al., 2015) with particular regard to the use of equivalent strut macro-models able to predict the panels combined IP/OOP response (Ricci et al., 2017 and Di Trapani et al., 2018). In 2015, Mosalam & Gunay developed a new macro-model (MG-model) with a single equivalent diagonal strut hinged at the ends and with a central inelastic section whose fibres were Out-Of-Plane aligned. The fibres withstand to the axial forces as well as to bending moment, allowing the IP/OOP interaction. A detailed state-of-art summary of the macro-models available in literature is reported in Asteris et al. (2017).

The following research aims to the evaluation of the performance of strengthened masonry infills compared to unreinforced panels and, in detail, the effectiveness of three external solutions (i.e. type F, FB and RBB already discussed in Minotto et al., 2019) on the overall behaviour of RC infilled frames by means of several F.E. non-linear analysis. The first step of the present paper is the development of a new macro-model able to predict the interaction between IP and OOP responses in case of TURM and TRM masonry infills. The numerical macro-model was characterized by two nonlinear fibre struts along each diagonal direction with a central fibre section oriented in the OOP direction and it was calibrated through the combined IP/OOP experimental results of unreinforced (Calvi and Bolognini, 2001) and strengthened thin masonry infills (Minotto et al., 2019). The second step of the activity consists in the carrying out of parametric non-linear static analyses which were performed on typical traditionally and seismically designed RC frame buildings. At this purpose, different frame configurations (squat, regular and slender) were assumed applying two In-Plane force distributions and simultaneous static forces acting on the panels in the OOP direction, defined according to the current Italian Code (Circolare 21<sup>st</sup> January 2019, n.7) and for increasing values of Peak Ground Acceleration (PGA). The benefits given by the proposed strengthening solution, especially for solution type F, are shown in terms of improvement of the overall structural response avoiding the anticipation of the infill Limit States and ensuring a limited damage distribution of masonry panels along building height. Finally, the new Italian Seismic Classification procedure according to D.M. 65, 7<sup>th</sup> March 2017 was implemented to evaluate the reduction of the expected annual losses, as well as of the seismic Risk Class of the buildings.

## 2 FINITE-ELEMENT MODELLING

### 2.1 RC frame numerical model

For an accurate calibration of the proposed infill macro-model, a detailed modelling of the RC frame was implemented. All RC beam and column elements were modelled in OpenSees (McKenna et al., 2007) using force-based beam-column elements with non-linear fibre sections. Each element was discretized into confined and not confined regions to consider the different stirrups spacing and the related confinement effects (increment of the concrete core peak compressive strength) were evaluated analytically through the implementation of the Mander's theory (Mander et al., 1988). A detailed representation of the RC frame numerical model is shown in Figure 1. The materials stress-strain relationships were chosen from the OpenSees library:

- *Concrete02* for cover and core concrete (based on Kent and Park, 1971).
- *Steel02* for reinforcing steel bars (based on Menegotto and Pinto, 1973).

Concrete and steel material constitutive laws were calibrated to fit the bare frame (BF) numerical response on the experimental one. The planar RC frame model presents fictitious OOP elastic springs characterized by OOP infinite stiffness placed on the frame joints to confer a realistic OOP stiffness. Finally, the modelling of the RC frame was completed introducing IP inertial masses lumped at each beam-column joint and which include both the frame masses and the infill ones.

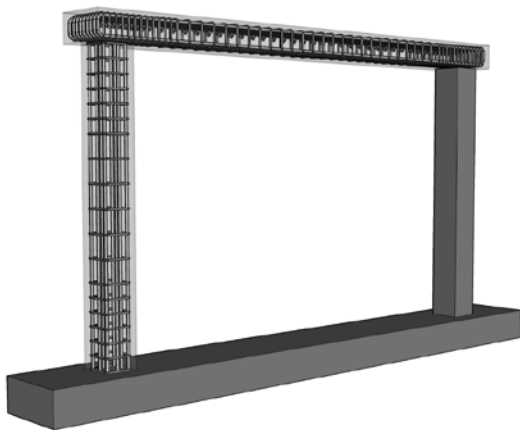


Figure 1. Representation of the RC frame numerical model.

### 2.2 Masonry infills macro-model

As stated before, the present research focused initially on the development of a macro-model able to simulate the interaction between the In-Plane and the Out-Of-Plane response of thin

masonry infills characterized by external reinforcing interventions. Firstly, two equivalent struts along each infill diagonal direction were implemented to better estimate the stresses distribution on the RC columns (Crisafulli, 1997).

Each equivalent strut was hinged to the RC frame and the two struts aligned along the same diagonal direction were spaced assuming a contact length appropriately calculated according to Stafford Smith (1966) and characterized by a triangular distribution of stresses. All struts have a central inelastic fibre section Out-Of-Plane oriented with 120 fibres symmetrically placed with respect to the strut axis. The fibres properties (i.e. area  $A_i$ , location  $z_i$ , and yielding strength  $f_{yi}$ ) were calculated through an IP/OOP (Axial Force/Bending Moment) domain defined as follows:

$$\left(\frac{P_N}{P_{NO}}\right)^{3/2} + \left(\frac{M_N}{M_{NO}}\right)^{3/2} \leq 1 \quad (1)$$

where  $P_{NO}$  and  $M_{NO}$  are respectively the IP and the OOP capacities calibrated on the experimental results. In case of MG-model, the above-mentioned parameters were calculated according to the FEMA-356 (2000). The masonry strength and stiffness degradations were taken into account by the implementation of the uniaxial trilinear Hysteretic material from the OpenSees library. In detail, in case of strengthened infills, the fibre section presented some external fibres which were calibrated using the Hysteretic stress-strain law with different material properties. In this way the inner fibres were calibrated for the unreinforced masonry material whereas the external ones to simulate the contribution of the reinforcement. This modelling approach was useful to increase the controllability of the model for the following calibrations on the experimental results of combined IP/OOP tests.

Due to the negligible tensile behaviour of masonry and to the configuration of the macro-model, it was necessary to decouple the IP response of the struts along the two diagonal direction in order to activate only the compressed struts. At this scope, the Hysteretic material laws of internal fibres are represented only by the compression envelope branch. In the OOP direction, all four struts were linked together by implementing an EqualDOF constraint.

The proposed macro-model is shown in the following Figure 2. The collapse condition of the infill and thus its removal from the frame numerical model was represented by an

appropriate removal domain (Collapse Limit State - CLS - domain) in terms of IP-drift vs. OOP-displacements.

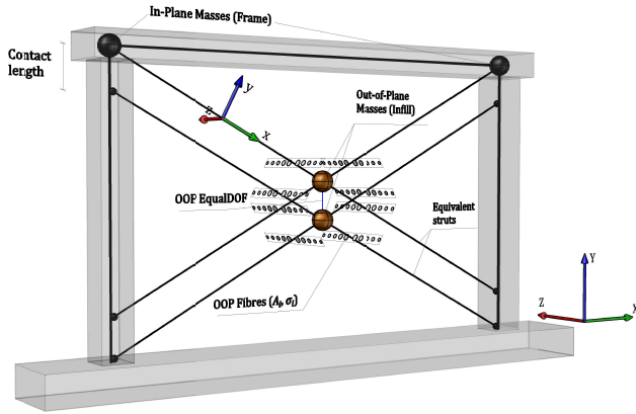


Figure 2. Representation of the proposed masonry infill macro-model.

To assess the combined IP/OOP damage level reached by the infill during the analyses, similar displacement domains at the Damage and the Ultimate Limit States (DLS and ULS) were introduced. All these domains were calibrated on the combined IP/OOP experimental test results by interpolating the OOP displacements to achieve the specific LS, which are function of the IP damage, and limiting it to the maximum IP drift of the reference Limit State. These experimental IP/OOP domains are shown in the next section 3.

Lastly, the masonry infill macro-model was completed introducing the Out-Of-Plane infill total mass which was equally divided and concentrated in the central nodes of all struts.

### 3 NUMERICAL CALIBRATION

The implementation of the proposed macro-model in the following parametric non-linear static analyses framework requested the calibration on the combined IP/OOP tests results. To evaluate the benefits given by the strengthening solutions experimentally studied at the Laboratory of the University of Padova, the proposed macro-model was initially calibrated on the results of an unreinforced thin masonry infill (Calvi and Bolognini, 2001) assumed as reference specimen (in the following shortly named URM). In case of strengthened infills, the macro-model was calibrated for three different strengthening solutions as follows.

- *Type F*: glass fibre plaster (M5) applied both sides of the infill wall;
- *Type FB*: glass fibre plaster applied both sides of the infill wall with the embedding of a bidirectional basalt grid;

- *Type RBB*: existing plaster with poor mechanical properties (M2.5, both sides) reinforced with external bidirectional basalt grid embedded into a plaster of good mechanical properties (M10).

Further details on the experimental tests are available in Minotto et al. (2019). Firstly, it was performed the In-Plane calibration of the bare frame configurations assuming the following material properties for the concrete and the reinforcing steel (Table 1). The calibrated In-Plane hysteretic loops are shown in the following Figure 3.

Table 1. Calibration parameters of RB bare frame for the two types of masonry infills (URM and TRM).

	URM (Calvi and Bolognini, 2001)	Strengthened (Minotto et al., 2019)
$f_{cm,col}$ [MPa]	28.4	38.3
$f_{cm,beam}$ [MPa]	33.7	24.4
$E_c$ [MPa]	27'080.0	20'136.6
$f_{ym}$ [MPa]	400.0	250.0
$E_y$ [MPa]	200'000.0	145'000.0

The second step of the activity concerned the calibration of the infill macro-model in terms of IP cyclic and OOP monotonic responses (the last one for different In-Plane damage levels). In the following Figure 4 is shown the calibration of the only URM infill. The calibration of all the strengthened infill walls was available in Donà et al. (2019).

The final step of the calibration procedure consisted in the definition of the experimental IP drift/OOP displacement domains corresponding to the infill Limit States. Observing the experimental OOP capacity curves of URM and strengthened infills, it was observed a stiffness and strength degradation due to the IP damage. As shown in Donà et al. (2019), the Out-Of-Plane infill Limit States were identified on the OOP capacity curves as follows.

- Damage Limit State (*DLS*) corresponding to the peak strength on the IP undamaged curve;
- Ultimate Limit State (*ULS*), corresponding to the peak strength on the IP damaged curve;
- a Collapse Limit State (*CLS*), which identifies the moment (determined also by experimental evidences) of sudden strength degradation, which anticipates the out-of-plane collapse of the panel.

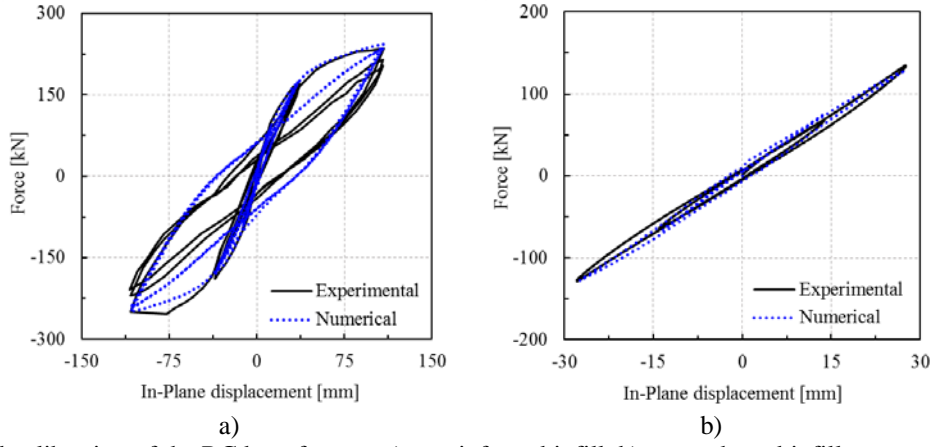


Figure 3. Numerical calibration of the RC bare frames: a) unreinforced infill, b) strengthened infills.

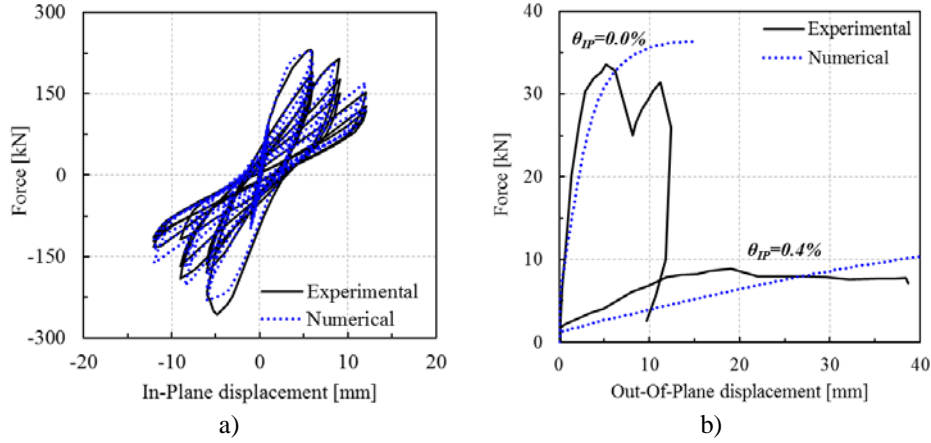


Figure 4. Numerical calibration of the URM infills: a) IP cyclic response, b) OOP monotonic response.

Table 2 lists the OOP maximum displacements at each Limit States and in case of ULS and CLS the linear interpolating equations are reported as function of the In-Plane drift  $\theta_{IP}$ . Conversely, the In-Plane Limit States were derived by the experimental infill envelope curve without the contribution of the RC frame. These values are reported in Table 3. The comparison of the values listed in the previous tables confirms that the application of the proposed strengthening solutions has negligible effects on the IP response at DLS and ULS. All infill walls reached their peak strength at an IP drift level around 0.25-0.30% and the Ultimate Limit State (corresponding to a strength degradation of 20% respect to the maximum capacity) at a drift level of 0.50%. The effect of the external reinforcing is underlined in the Out-Of-Plane capacity of the infills. In particular, the Damage Limit State occurs for higher values of OOP displacement respect to the URM infill.

For the sake of simplicity, the following Figure 4 shows the definition of the IP drift/OOP displacement domains (DLS, ULS and CLS) only in case of URM infill. The same domains were defined in case of strengthened infill walls and reported in Donà et al. (2019).

Table 2. Infill Out-Of-Plane displacement limits at Damage, Ultimate and Collapse Limit States (unit *mm*).

Limit State	DLS	ULS	CLS
<b>URM</b>	5.10	$16.50\theta_{IP}+6.40$	$30.00\theta_{IP}+8.00$
<b>F</b>	14.60	$6.25\theta_{IP}+16.00$	$7.08\theta_{IP}+17.50$
<b>FB</b>	5.35	$5.17\theta_{IP}+7.34$	$5.54\theta_{IP}+9.53$
<b>RBB</b>	12.00	$6.28\theta_{IP}+13.11$	$6.19\theta_{IP}+14.49$

Table 3. Infill In-Plane drift limits at Damage, Ultimate and Collapse Limit States (unit %).

Limit State	URM	F	FB	RBB
DLS	0.30	0.30	0.30	0.25
ULS	0.50	0.50	0.50	0.50
CLS	1.00	1.50	1.50	1.50

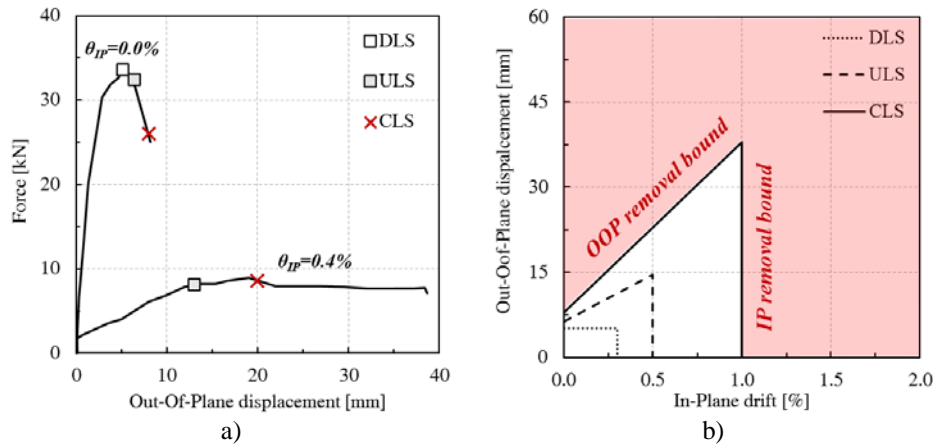


Figure 5. URM infill walls: a) Identification of the infill experimental OOP Limit States and b) IP drift vs. OOP-displacement domains for all Limit States.

## 4 PARAMETRIC NON-LINEAR STATIC ANALYSES

### 4.1 Framework description

The previous calibrated macro-models for URM and TRM infills were implemented in the following parametric non-linear static analyses. The framework consists of combined IP/OOP pushover analysis carried out on several RC frame configurations defined as squat, regular and slender as function of the ratio between the number of storeys and bays. All the implemented buildings were shortly name as “ $n \times m$ ” where  $n$  is the number of bays and  $m$  the number of storeys. The following RC frame configurations were investigated: 4x2, 2x3, 1x3, 2x6. The above-mentioned buildings stock represents typical Italian and European RC infilled frames and was specifically designed only for gravity loads (Traditional Design - TD) and for lateral seismic forces (Seismic Design - SD). The aim of this design approach consists in the desire to verify the benefits of the infills retrofit in case of existing (TD) and new (SD) buildings.

For design purposes, steel type B450C and a concrete C30/37 were used according to Italian Code NTC2018 in case of SD buildings. Conversely, TD frames were characterized by steel type AQ50-60 and concrete C20/25 according to common Italian design criteria of the 50-80s (Verderame et al., 2001 and Cristofaro et al., 2011). The design of the RC frame was performed considering the variability of the column sections every three storeys. The length of bays and the height of storeys were chosen

assuming the geometrical dimensions of the experimental masonry infills.

The non-linear static analyses were carried out on both the BF and infilled frame (IF) configurations by applying IP and OOP load patterns chosen according to the Italian Code NTC2018. Two incremental In-Plane patterns were applied on the RC frame.

- *Distribution Gr1\_a*: proportional to masses and heights.
- *Distribution Gr2\_a*: uniform distribution of accelerations along the height of the structure.

The Out-Of-Plane demand, necessary for the evaluation of the combined IP/OOP effects on masonry infills, follows the formulation for non-structural elements:

$$F_a = \frac{S_a W_a}{q_a} \quad (2)$$

where  $F_a$  is the horizontal seismic force acting on the masonry infill centre of mass,  $S_a$  is the spectral acceleration acting on the infill wall,  $W_a$  is the wall weight and  $q_a$  is the element behaviour factor (assumed as 2). The maximum spectral acceleration  $S_a$  was defined according to the simplified formulation for RC frame buildings available in Circolare 21<sup>st</sup> January 2019, n.7 (C7.2.3, formula C7.2.11). Three values of  $a_g S$  equal to 0.10g, 0.20g and 0.30g were chosen for the OOP demand. The intensities of the OOP forces were updated step by step during the analysis to consider the influence of the IP damage (planar deformability of the frame) on the increase of the infills period  $T_a$  at each storey. Analytical piecewise functions which represent the relationship between  $T_a$  and IP drift were calibrated on the experimental results of the combined IP/OOP tests (see Figure 5).

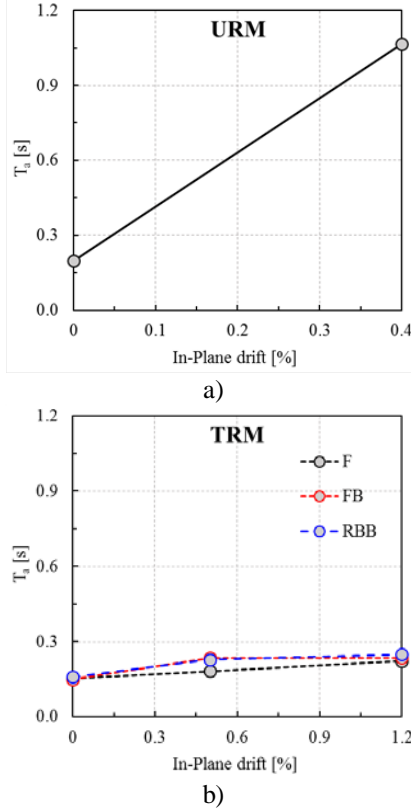


Figure 5. Piecewise linear functions for the evaluation of the OOP vibration period  $T_a$  as function of the IP drift level: a) unreinforced and b) strengthened masonry infills.

In case of BF, pushover analyses were carried out In-Plane whereas in case of IF configurations two different simulations were conducted by investigating both the only IP and the combined IP/OOP responses of the infilled buildings.

#### 4.2 Performance Levels and Limit States

For the evaluation of the structural damages on both RC frame and masonry infills, several Performance Levels (PLs) and Limit States (LS) were introduced and checked step by step during the analysis. The RC frame Performance Levels are listed below.

- *colYM* (column Yield bending Moment)
- *colUM* (column Ultimate bending Moment)
- *beamYM* (beam Yield bending Moment)
- *beamUM* (beam Ultimate bending Moment)
- *colSF* (column Shear Failure)
- *beamSF* (beam Shear Failure)
- *colNF* (column Nodal Failure)
- *ISDR* (Inter-Storey Drift Ratios)

The Yield and Ultimate bending moments of columns and beams were checked by implementing analytical functions which correlate the yield and ultimate curvatures,  $\chi_y$  and  $\chi_u$  respectively, to the acting axial load. These functions were obtained by preliminary parametric moment-curvature analyses conducted

on the structural member sections for incremental values of the vertical axial load  $N$ . Step by step during the analysis, the actual curvatures of all RC members sections were compared to the expected ones from analytical expressions. Typical analytical functions of  $\chi_y$  and  $\chi_u$  are shown in the following Figure 6 for both Seismic and Traditional sections.

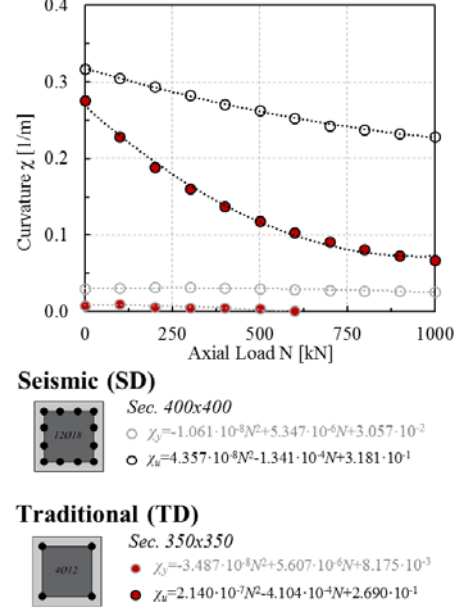


Figure 6. Example of typical nominal  $\chi_y$  and ultimate  $\chi_u$  curvatures as function of the acting axial load  $N$ .

The shear capacity of the RC columns and beams was evaluated through the formulation proposed by Sezen (2002) whereas the node rotation capacity was defined according to the formulations proposed in Circolare 21<sup>st</sup> January 2019, n.7. . Finally, many reference Inter-Storey Drift Ratios (e.g. 0.3%, 0.5%, 1.0%, etc.) were assumed.

The Damage and Ultimate Limit States of the frame are therefore defined as follows.

$$frDLS = \min \{ colYM; ISDR = 0.5\% \}$$

$$frULS = \min \left\{ \begin{array}{l} beamUM; colUM; colSF; colNF; \\ ISDR = 2.0\% \end{array} \right\} \quad (3)$$

The infill IP drift/OOP displacement domains previously described and calibrated were implemented in the analysis procedure to evaluate the progression of the infill damages.

#### 4.3 Seismic input

The application of the OOP pattern on non-structural elements was performed for three values of  $a_g S$  equal to 0.10g, 0.20g and 0.30g. The execution of the following post-processing analyses for the evaluation of the infill damage

distribution and building Risk Classes requested the definition of the corresponding spectra. The seismic demand shape was defined, for each  $a_g S$  intensity, following the formulation available in NTC2018 assuming a soil type B, structural Class of use II and Nominal Life of the building equal to 50 years. The parameters  $a_g$ ,  $F_0$  and  $T_C^*$  were assumed as average values on the Italian territory. The following Figure 7 summarizes the at Damage and Ultimate Limit State spectra calculated for a return period of 50 years and 475 years respectively.

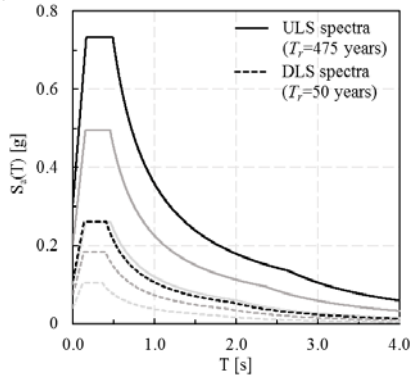


Figure 7. DLS and ULS seismic spectra.

#### 4.4 Force-displacement curves

Among the main outputs of the parametric non-linear static analyses, the capacity curves represent a preliminary result useful for the

evaluation of the infills contribution on the overall building response. Pushover curves are shown in terms of the total IP base shear force versus the maximum displacement reached at the control node placed at the top of the building. The following Figure 8 and Figure 9 show the comparison of the capacity curves in case of frame 2x3 (Seismic and Traditional Design respectively) with unreinforced and strengthened (i.e. solution type F) thin masonry infills. In the charts, the solid red curves represent the response of the IF configuration in case of combined IP/OOP seismic action for three intensities of  $a_g S$  in the Out-Of-Plane direction. The Performance Levels and the Limit States reached by the RC frame and masonry infills are shown along each capacity curve. The principal outcomes from the pushover curves are summarized below.

The type of design greatly affects the RC frame overall response. The design for horizontal seismic loads improves the yield and ultimate capacity of the structure. In particular, the yield strength ratio between SD and TD frames is variable between 2.5 and 5 depending on the configuration. The strength ratio at  $frULS$  is variable between 2 and 2.5.

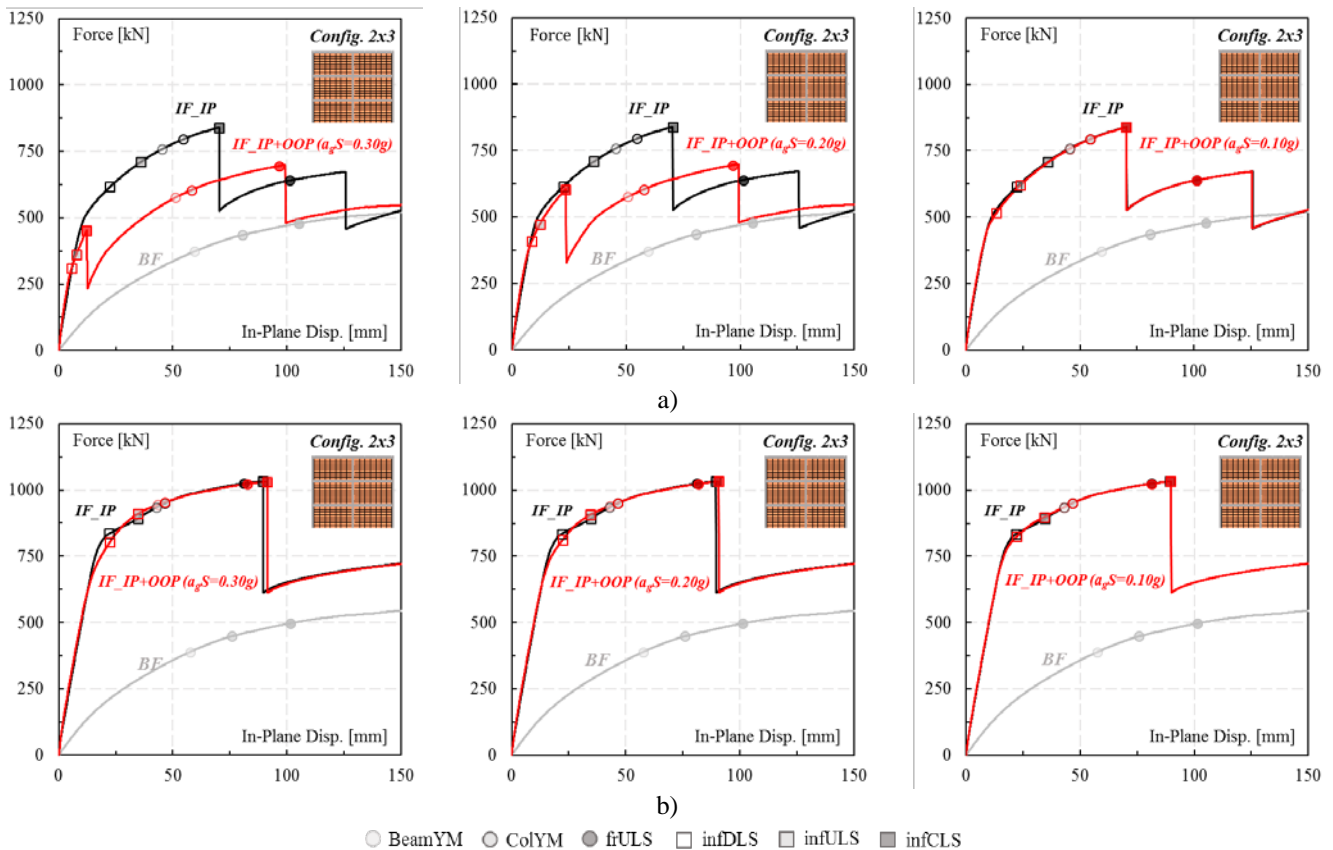


Figure 8. Capacity curves of RC frame configuration 2x3 and Seismic Design: a) URM infill, b) strengthened infill type F.

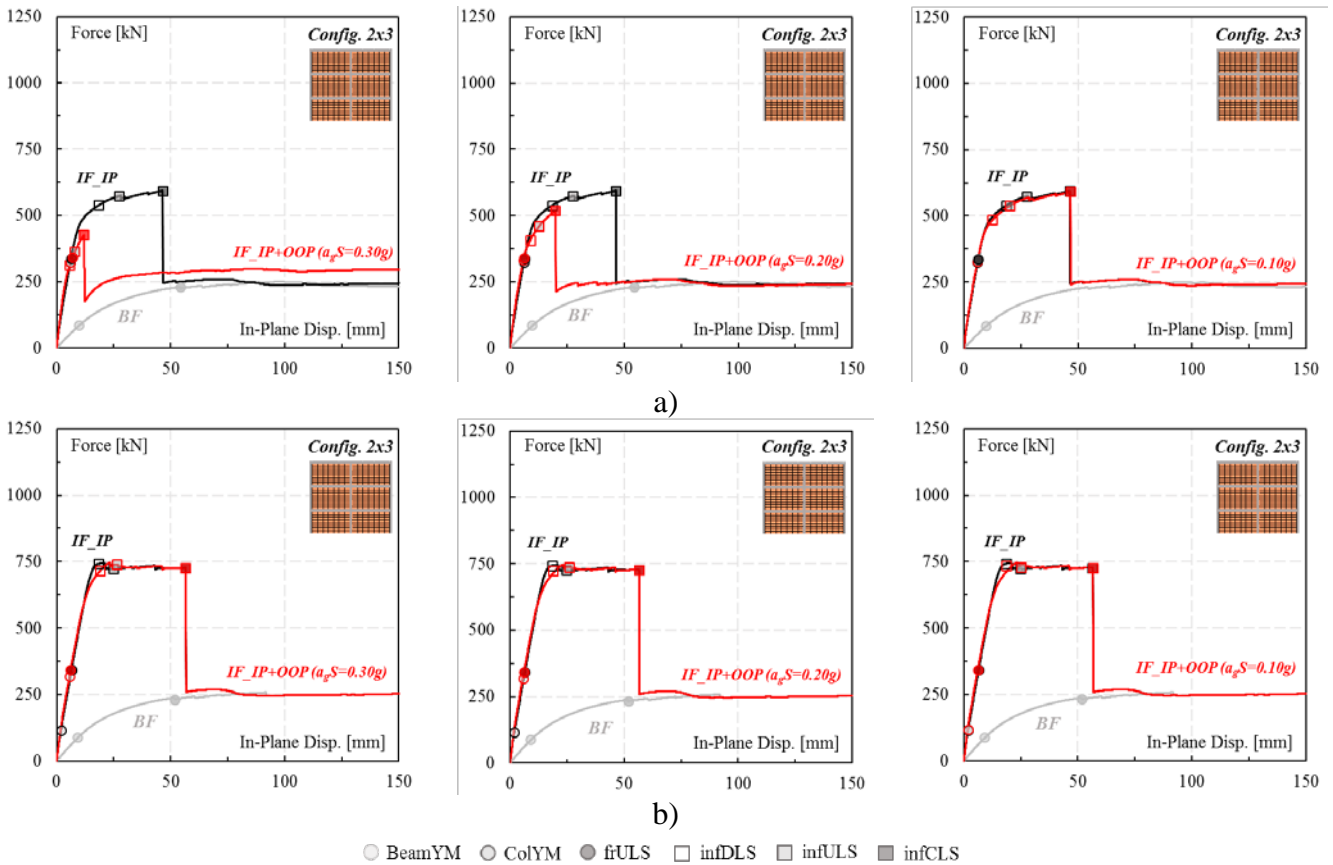


Figure 9. Capacity curves of RC frame configuration 2x3 and Traditional Design: a) URM infill, b) strengthened infill type F.

The infill wall contribution on the IP overall capacity of the infilled frame is represented by the maximum distance between the IP curve and the BF one and it increases as the number of bays rises (i.e. squat configurations). Furthermore, URM and strengthened infills provide different contributions. Strengthened infills are responsible of a strength increment of 40÷80% compared to URM infills. The lower and the upper bounds are related to the F and RBB solutions respectively. Lastly, the design type affects the intensity of the infill contribution. In particular, it is greater in case of SD frames with a maximum increment of 20% respect to TD buildings. In fact, the Seismic Design of the RC frame guarantees a better distribution of the seismic action along the building height exploiting the upper floor panels.

The extension of the capacity curve branch until the reaching of the first infill collapse point (*infCLS*) is greater in the case of strengthened infills thanks to combined IP/OOP removal domains which allow greater IP maximum displacement (see Table 3). It is noteworthy that, in the range of the investigated Out-Of-Plane PGAs, the collapse of the strengthened infills is governed by the reaching of the IP capacity.

The infill strut action anticipates the *colYM* and the *frULS* both in case of URM and

strengthened infills. In case of TD frames, the brittle shear failure of the vertical members was observed. This kind of damage is located at the external (not confined) RC joint.

The effectiveness of the above-mentioned strengthening solutions was demonstrated by the capacity curves of the infilled frame subjected to combined IP/OOP seismic action. Until the OOP  $a_gS=0.30g$ , no early infill collapse was observed. Conversely, URM infill wall proved to be very vulnerable to the OOP seismic action. In fact, all the infill Limit State, in particular the *infCLS*, anticipate as the PGA increases (contrary to what was observed in the case of strengthened infills). These observations are valid both in case of SD and TD frames and, in general, regardless of the structural configuration. In case of squat configurations (e.g. 4x2), the OOP action is responsible of the anticipation of the URM infill LS, as just stated, but the collapse of the panels is governed by their IP damage (due to a lower intensity of the OOP seismic action related to the reduced height of the squat buildings).

Further observations concerning the different strengthening solutions are available in Donà et al., 2019.

#### 4.5 Inter-Storey Drift profiles

Figure 10 shows the IP inter-storey drift profiles in case of 2x3 and 2x6 frames with Traditional Design at infill Damage and Ultimate Limit States and at frame Ultimate Limit State. This representation is useful to evaluate the masonry infills damage distribution along building height and it was obtained as the envelope of the profiles corresponding to the two analysed IP distributions (i.e. Gr1\_a and Gr2\_a) assuming at each storey the major drift.

The following drift profiles confirm all the observations derived from capacity curves. In detail, it was observed that the OOP action has a relevant effect as anticipation of the *infDLS* and *infULS* in case of URM masonry panels. The use of external strengthening solutions avoids the occurrence of this behaviour.

A further interesting issue concerns the distribution of the infills damage along the building height. In detail, in case of slender buildings (e.g. 2x6), the first damages were observed at the second storey due to the combination of the IP and OOP damage of the masonry panels. At the *infULS*, a significant damage distribution occurred at all the intermediate storeys (until the 4<sup>th</sup> level). Conversely, the damage of non-structural elements is concentrated on the ground floor in the case of buildings of lesser height (e.g. 2x3, 4x2, etc.).

In terms of Ultimate Limit State of the RC frame, it is noteworthy that, both in case of URM and strengthened infills, a significant anticipation of the *frULS* was observed caused by the shear failure of the columns which occurred on the external not-confined beam-column joints. This behaviour is demonstrated by the *frULS* drift profiles which are closed to the ordinate axis. It follows that the retrofit strategies of the infills improve the structural response avoiding the collapse of the infills but it is not able to prevent the failure of the structural members which require specific and adequate retrofit solutions.

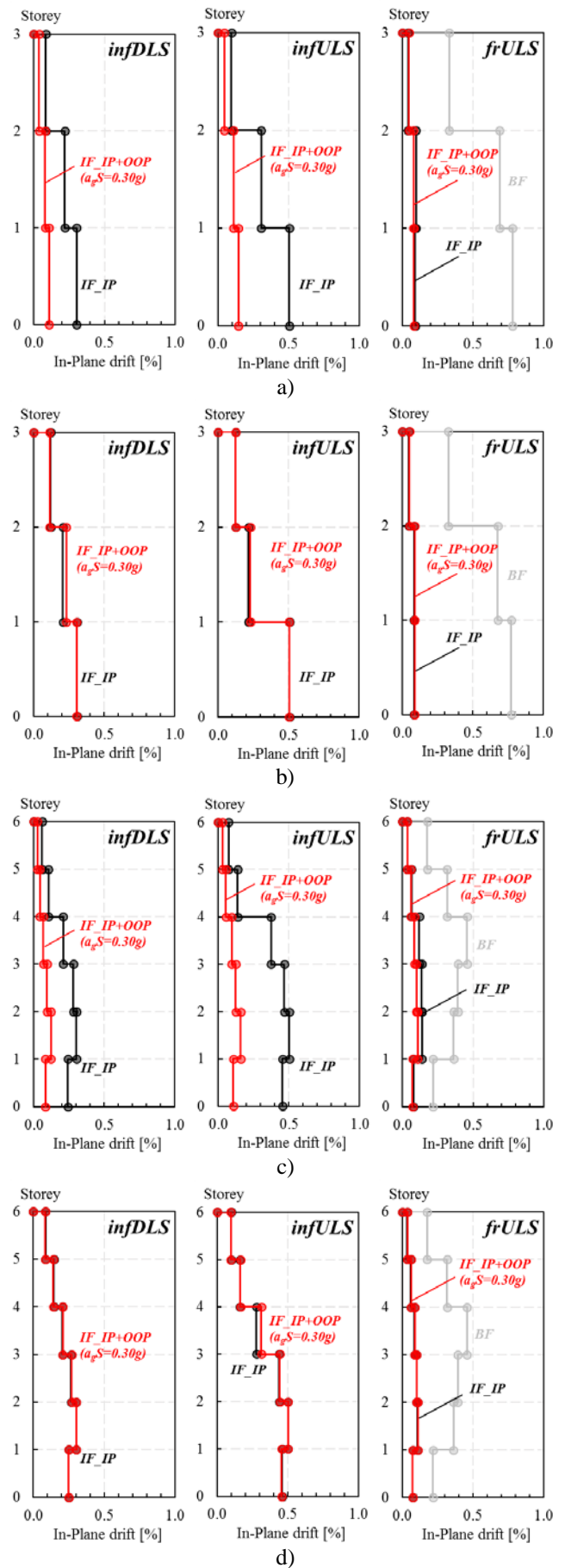


Figure 10. Drift profiles at both infill and frame Limit States: a) 2x3 TD URM infill, b) 2x3 TD strengthened infill type F, c) 2x6 TD URM infill and d) 2x6 TD strengthened infill type F.

#### 4.6 Damage distribution on masonry infills

The improvement of the URM infill performance given by the strengthening solutions is demonstrated by the following Figure 11 which shows the infill damage distributions for three values of PGA (i.e.  $a_g S=0.10g$ ,  $a_g S=0.20g$  and  $a_g S=0.30g$ ). The evaluation of the damages on masonry infills required the implementation of the procedure proposed by Cattari and Lagomarsino (2012) - “Perpetuate”, for the determination of the intersection point between the capacity curve of the infilled frame and the demand spectrum which was represented by the ULS spectrum (see Figure 7) for a specific value of PGA. A detailed description of the procedure is available in Donà et al. (2017). Comparing the above-mentioned performance point with the order of infill Limit States recorded step by step during the numerical analysis, it was possible to identify the panels damage pattern along building height.

It was observed that, both in case of SD and TD frames, the combined IP/OOP seismic action damages the URM infills starting from low values of  $a_g S$  with a more relevant impact as the height of the building increases (see configuration 2x6). The strengthening of the masonry panels allows the improvement of the OOP capacity with a substantial reduction of the infill damages.

It is noteworthy that existing buildings (i.e. Traditional Design) cannot withstand the most intense seismic action and, in detail, the seismic demand with  $a_g S=0.30g$  is responsible of the global collapse of the RC frame. The result confirms that the strengthening of the masonry infills should be carried out together with the retrofit of the RC structural elements to obtain a significative improvement of the building overall performance.

#### 4.7 Evaluation of the Building Risk Class

The final step of the present research consists in the evaluation of the building Risk Class according to the new Italian Seismic Classification procedure (D.M. 65, 7<sup>th</sup> March 2017). Two parameters are necessary for the calculation of the Risk Class. The first is the expected average annual loss (shortly named PAM), which takes into account the economic losses associated to the damage of structural and non-structural elements, and related to the reconstruction cost (CR) of the building neglecting its contents. The reconstruction costs are defined in the following Table 4.

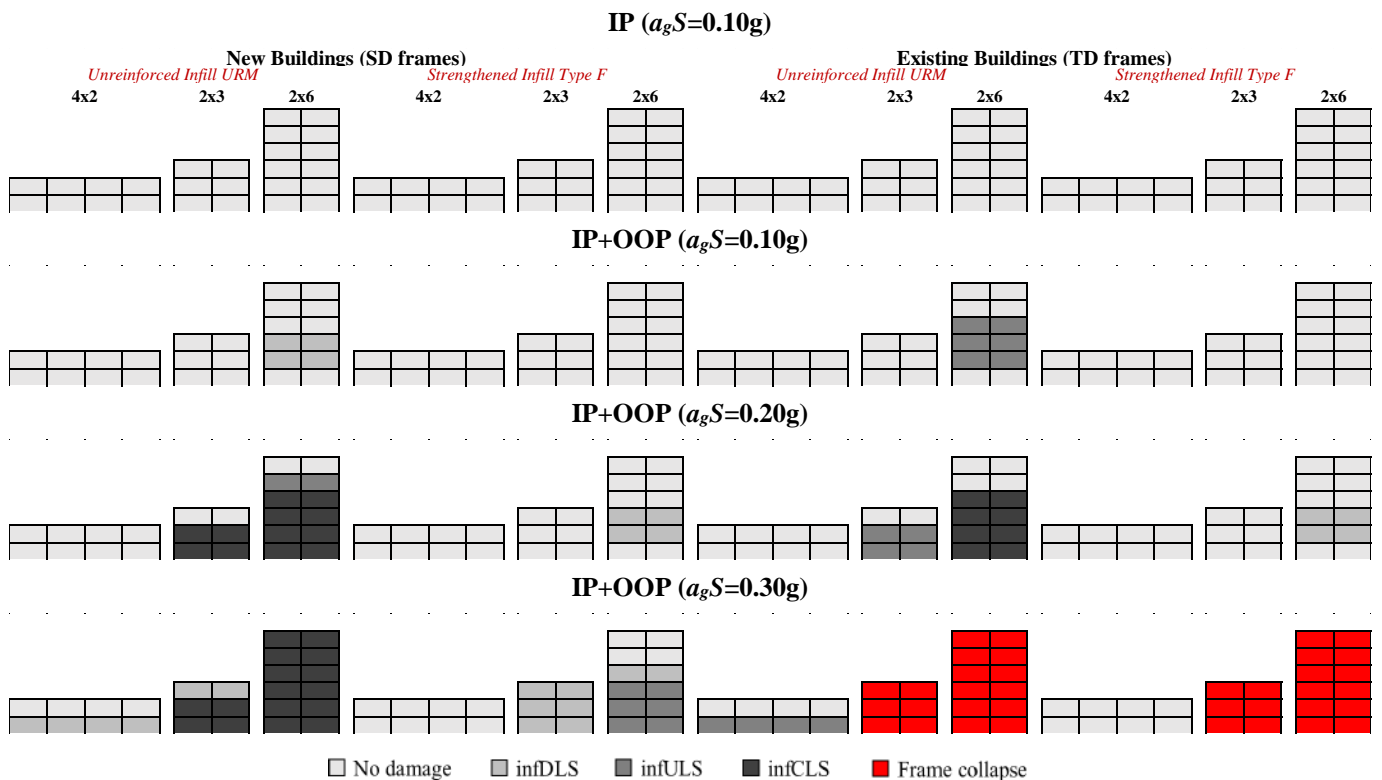


Figure 11. Damage distribution on masonry infills in case of SD and TD frames for IP and combined IP/OOP actions.

Table 4. Building reconstruction costs at each Limit State.

Limit State	IDLS	OLS	DLS	ULS	CLS	RLS
CR [%]	0	7	15	50	80	100

Note: IDLS=Initial Damage Limit State; OLS=Operational Limit State; DLS=Damage Limit State; ULS=Ultimate Limit State; CLS=Collapse Limit State; RLS=Reconstruction Limit State.

The second parameter is the safety index at the Ultimate Limit State (IS-V) defined as the ratio between the capacity and demand in terms of PGA at the Ultimate Limit State. The IS-V safety index is better known as Risk Index.

The procedure for the calculation of the PAM index follows the next steps.

1. Execution of the numerical analyses and evaluation of the capacity in terms of PGA at DLS and ULS. For the following analyses, the DLS was assumed as the *infDLS* whereas the ULS as the *frULS*.
2. Calculation of the capacity return period corresponding to each Limit State as follows.

$$T_{rC} = T_{rD} \left( \frac{PGA_C}{PGA_D} \right)^\eta \quad (4)$$

where  $T_{rC}$  is the return period of the capacity,  $T_{rD}$  is the return period of the demand,  $PGA_C$  and  $PGA_D$  are the capacity and the demand respectively and  $\eta$  a coefficient which is function of  $a_g$ . In a simplified way it can be assumed as 1/0.49. The capacities at *infDLS* and *frULS* were obtained by implementing the procedure proposed by Cattari and Lagomarsino (2012) and described in Donà et al., 2017.

3. Calculation of the annual average frequency of exceedance  $\lambda$  at each Limit State defined in Table 4. The capacity corresponding to the Operational and Collapse Limit States were assumed in a simplified way as  $\lambda_{OLS}=1.67\lambda_{DLS}$  e  $\lambda_{CLS}=0.49\lambda_{ULS}$ . In addition, the Reconstruction Limit State has the same  $T_r$  of the CLS and the Initial Damage Limit State occurs for a return period of 10 years. Associating each Reconstruction Cost to the corresponding  $\lambda$  at each Limit State it is possible to define a linear piecewise function and the area under the curve represents the PAM index. An example of PAM curve is shown in Figure 12.
4. Calculation of the IS-V index as the ratio between the capacity and the demand at *frULS*.
5. Definition of the PAM and IS-V classes according to the following Table 5 and Table 6. The building Risk Class is defined as the worst condition between PAM and IS-V classes.

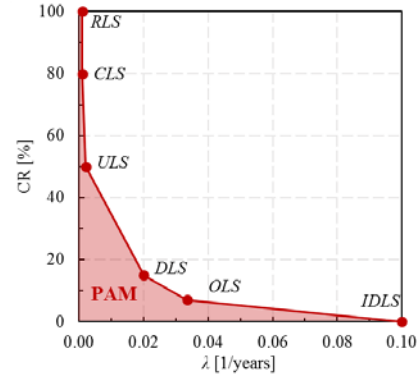


Figure 12. Example of the linear piecewise function for the calculation of the PAM index.

Table 5. PAM classes.

PAM index	PAM class
$PAM \leq 0.50\%$	$A^+_{PAM}$
$0.50\% < PAM \leq 1.00\%$	$A_{PAM}$
$1.00\% < PAM \leq 1.50\%$	$B_{PAM}$
$1.50\% < PAM \leq 2.50\%$	$C_{PAM}$
$2.50\% < PAM \leq 3.50\%$	$D_{PAM}$
$3.50\% < PAM \leq 4.50\%$	$E_{PAM}$
$4.50\% < PAM \leq 7.50\%$	$F_{PAM}$
$7.50\% \leq PAM$	$G_{PAM}$

Table 6. IS-V classes.

IS-V index	IS-V class
$IS-V \geq 100\%$	$A^+_{IS-v}$
$80\% \leq IS-V < 100\%$	$A_{IS-v}$
$60\% \leq IS-V < 80\%$	$B_{IS-v}$
$45\% \leq IS-V < 60\%$	$C_{IS-v}$
$30\% \leq IS-V < 45\%$	$D_{IS-v}$
$15\% \leq IS-V < 30\%$	$E_{IS-v}$
$IS-V \leq 15\%$	$F_{IS-v}$

In the following Table 7 and Table 8 are listed the building Risk Classes calculated in case of SD and TD frames respectively and considering URM and strengthened thin masonry infills (solution type F). Considering the most relevant case of existing buildings, the *frULS* is affected by the shear failure of the RC external beam-column joints and in case of URM infills the building Risk Class is representative of a very vulnerable behaviour from the seismic point of view. In fact, the combined IP/OOP seismic action induces a significant anticipation of the infill damage (*infDLS*) with a subsequent increase of the PAM index and worsening of the associated Risk Class. It is noteworthy that, in this case studies, the building Risk Class is mainly constrained by the PAM class.

The strengthening of the infills, as stated before, improves the OOP capacity of the panels but further interventions are requested in

structural elements in order to avoid the occurrence of the brittle mechanisms. It follows that, also if the application of the wall external reinforcement allows a postponement of the *infDLS*, the benefits on the building Risk Class are limited. The combination of the infills retrofit with the confinement of all the RC external joints (prevention of the shear failure) allows a significative reduction of the building Risk Class. This conclusion is significative, above all in relation to what is stated in the D.M. 65, 7<sup>th</sup> March 2017. In fact, in case of RC frame buildings it is possible to assume (without specific numerical analyses) the transition to the next best Risk Class performing only the following interventions:

- retrofit of the masonry infills on the perimeter of the building to avoid the OOP collapse;
- confinement of all not-confined external RC beam-column joints;
- restoring of damaged and degraded areas.

The numerical results confirms that the retrofit of the URM masonry infills with the proposed strengthening solutions combined with the retrofit of the RC structural joints allow the improvement of the building Risk Class.

Table 7. Building Seismic Risk Class for different type of thin masonry infills and SD frames.

<i>SD</i>	URM		F	
	IP	IP+OOP	IP	IP+OOP
<b>4x2</b>	A+	A+	A+	A+
<b>2x3</b>	A	A	A+	A+
<b>2x6</b>	A	B	A	A

Table 8. Building Seismic Risk Class for different type of thin masonry infills and TD frames.

<i>TD</i>	URM		F	
	IP	IP+OOP	IP	IP+OOP
<b>4x2</b>	C	C	A+	A+
<b>2x3</b>	C	C	B	B
<b>2x6</b>	F	F	B	A

## 5 CONCLUSIONS

The present research activity focused on the development of a masonry infill macro-model able to predict the combined IP/OOP response in case of URM and strengthened panels. The macro-model was initially calibrated on the results of combined IP/OOP experimental tests conducted on URM and strengthened thin masonry infills and subsequently it was implemented in an extended parametric non-linear static analyses to evaluate the benefits of the infill retrofit solutions on the overall response of the RC infilled frames. At this purpose, several structural configurations (squat, regular and slender) were specifically designed both in case of seismic and only gravity loads (i.e. SD and TD respectively). The numerical analyses were conducted considering IP incremental loads with two distributions of forces (i.e. Gr1\_a and Gr2\_a) and OOP forces acting on non-structural elements (according to Circolare 21<sup>st</sup> January 2019, n.7) with three level of  $a_g S$  (i.e. 0.10g, 0.20g and 0.30g).

The results of the analyses confirmed the effectiveness of the proposed strengthening solutions (i.e. type F) in terms of improvement of the OOP capacity. In the range on the investigated PGAs, the combined IP/OOP seismic action doesn't affect the overall response of the infilled frames and no anticipation of the infill Limit States was observed. In case of existing buildings (TD), the retrofit intervention of the masonry infills improves the structural response avoiding the collapse of the infills but it is not able to prevent the failure of the RC column-beam joints. The confinement of all not-confined external joints can be considered as an optimal retrofit intervention in order to prevent the brittle collapse of the structure also ensuring an improvement in the building Risk Class.

## REFERENCES

- Asteris, P.G., Cavaleri, L., Di Trapani, F., Tsaris, A.K., 2017. Numerical modelling of out-of-plane response of infilled frames: State of the art and future challenges for the equivalent strut macromodels, *Engineering Structures*, **132**, 110-122.
- Calvi, G.M., Bolognini, D., 2001. Seismic response of reinforced concrete frames infilled with weakly reinforced masonry panels, *Journal of Earthquake Engineering*, **5**, 153-185.
- Cattari, S., Lagomarsino, S., 2012. PERFORMANCE-based approach to Earthquake protection of cultural heritage in European and Mediterranean countries”.
- Circolare 21<sup>st</sup> Jan. 2019, n.7, *Istruzioni per l'applicazione dell'“Aggiornamento delle Nuove norme tecniche per le costruzioni”* di cui al D.M. 17 gennaio 2018.
- Crisafulli, F.J., 1997. Seismic behaviour of reinforced concrete structures with masonry infills, Ph.D. Thesis.
- Cristofaro, M. T., D'Ambrisi, A., De Stefano, M., Pucinotti, R., Tanganelli, M., 2011. Caratterizzazione meccanica di calcestruzzi estratti da edifici esistenti con il metodo sonreb, *Conferenza Nazionale sulle prove non Distruttive Monitoraggio Diagnostica, Associazione Italiana Prove non Distruttive Monitoraggio Diagnostica*, October 26-28, Florence, IT.
- D.M. 7<sup>th</sup> March 2017 n. 65, Sisma Bonus – Linee guida per la classificazione del rischio sismico delle costruzioni e i relativi allegati.
- Di Trapani, F., Shing, P.B., Cavaleri, L., 2018. Macroelement model for in-plane and out-of-plane responses of masonry infills in frame structures, *Journal of Structural Engineering (ASCE)*, **144**(2): 04017198.
- Dolšek, M., Fajfar, P., 2008. The effect of masonry infills on the seismic response of a four-storey reinforced concrete frame - a deterministic assessment, *Engineering Structures*, **30**, 1991-2001.
- Dolšek, M., Fajfar, P., 2001. Soft storey effects in uniformly infilled reinforced concrete frames, *Journal of Earthquake Engineering*, **5**, 1-12.
- Donà, M., Minotto, M., Bernardi, E., Saler, E., Verlato, N., da Porto, F., 2019. Macro-modelling of combined in-plane and out-of-plane seismic response of thin strengthened masonry infills, *7<sup>th</sup> International Conference on Computational Methods in Structural Dynamics and Earthquake Engineering (COMPdyn 2019)*, June 24-26, Crete, GR.
- Donà, M., Minotto, M., Saler, E., Tecchio, G., da Porto, F., 2017. Combined in-plane and out-of-plane seismic effects on masonry infills in RC frames, *Ingegneria Sismica - Anno XXXIV - Special Issue: Seismic Vulnerability of Structures and Infrastructures: Strategies for Assessment and Mitigation*.
- EN 1998-1: Eurocode 8. (2004). “Design of structures for earthquake resistance – Part 1: General rules, seismic actions and rules for buildings,” *European Committee for Standardization*, Brussels, Belgium.
- FEMA-356, 2000. Prestandard and Commentary for Seismic Rehabilitation of Buildings. *Federal Emergency Management Agency*, Washington DC.
- Hak, S., Morandi, P., Magenes, G., Sullivan, T.J., 2012. Damage Control for Clay Masonry Infills in the Design of RC Frame Structures, *Journal of Earthquake Engineering*, **16**, 1-35.
- Jeselia, C.M., Jayalekshmi, B.R., Venkataramana, K., 2013. Modeling of Masonry infills - A review, *American Journal of Engineering Research (AJER)*, **2**, 59- 63.
- Kent, D.C., Park, R., 1971. Flexural members with confined concrete, *Journal of the Structural Division*, **97**(7), 1969-1990.
- Mander, J.B., Priestley, M.J.N., Park, R., 1988. Theoretical Stress-Strain Model for Confined Concrete, *Journal of Structural Engineering*, **114**(8), 1804-1826.
- McKenna, F., Mazzoni, S., Scott, M. H., Fenves, G.L., et al. OpenSees, 2007. Open System for Earthquake Engineering Simulation, Pacific Earthquake Engineering Research Center, US, version 1.7.4, openses.berkeley.edu.
- Menegotto, M., Pinto, P.E., 1973. Method of analysis for cyclically loaded rc frames including changes in geometry and non-elastic behaviour of elements under combined normal force and bending, *IABSE Congress Reports of the Working Commission*, **13**, 15-22.
- Minotto, M., Verlato, N., Donà, M., Saler, E., da Porto, F., 2019. Strengthened thin clay masonry infills: In-Plane and Out-Of-Plane experimental tests, *13<sup>th</sup> North American Masonry Conference*, June 17-19, Utah, US.
- Mosalam, M., Khalid, M., Günay, S., 2015. Progressive collapse analysis of reinforced concrete frames with unreinforced masonry infill walls considering in-plane/out-of-plane interaction, *Earthquake Spectra*, **31**(2), 921-943.
- NTC2018, D.M. 17<sup>th</sup> January 2018, Norme Tecniche per le Costruzioni.
- Papanicolaou, C.G., Triantafyllou, T.C., Papathanasiou, M., Karlos, K., 2007. Textile reinforced mortar (TRM) versus FRP as strengthening material of URM walls: out-of-plane cyclic loading, *Materials and Structures*, **41**, 143-157.
- Ricci, P., Di Domenico, M., Verderame, G. M., 2017. Empirical-based infill model accounting for in-plane/out-of-plane interaction applied for the seismic assessment of EC8-designed RC frames, *6<sup>th</sup> International Conference on Computational Methods in Structural Dynamics and Earthquake Engineering (COMPdyn 2017)*, June 12-14, Rhodes Island, GR.
- Saatcioglu, M., Serrato, F., Foo, S., 2005. Seismic Performance of Masonry Infill Walls Retro-fitted With CFRP Sheets, *7<sup>th</sup> International Symposium of Fiber Reinforced Polymer Reinforcement for Reinforced Concrete Structures (FRPRCS-7)*, 341-351.
- Sezen, H., 2002. Seismic behavior and modeling of reinforced concrete building columns, Ph.D. Thesis.
- Smith, B.S., 1966. Behavior of square infilled frames, *Journal of the Structural Division*, **92**(1), 381-404.
- Tarque, N., Candido, L., Camata, G., Spacone, E., 2015. Masonry infilled frame structures: state-of-the-art review of numerical modelling, *Earthquakes and Structures*, **8**(3), 733-759.
- Tumialan, J.G., Galati, N., Nanni, A., 2003. Fibre-Reinforced Polymer Strengthening of Unreinforced Masonry Walls Subject to Out-of-Plane Loads, *American Concrete Institute Structural Journal*, **100**, 321-329.
- Valluzzi, M.R., da Porto, F., Garbin, E., Panizza, M., 2014. Out-of-plane behaviour of infill masonry panels strengthened with composite materials, *Materials and Structures*, **47**, 2131-2145.
- Verderame, G.M., Manfredi, G., 2001. Le proprietà meccaniche dei calcestruzzi impiegati nelle strutture in cemento armato realizzate negli anni '60, X Convegno ANIDIS, September 9-13, Potenza/Matera, IT.